

Temporal Graph Functional Dependencies [Extended Version]

Morteza Alipourlangouri
McMaster University
alipoum@mcmaster.ca

Adam Mansfield, Fei Chiang
McMaster University
{mansfa2, fchiang}@mcmaster.ca

Yinghui Wu
Case Western Reserve University
yxw1650@case.edu

Abstract—Data dependencies have been extended to graphs to characterize topological and value constraints. Existing data dependencies are defined to capture inconsistencies in static graphs. Nevertheless, inconsistencies may occur over evolving graphs and only for certain time periods. The need for capturing such inconsistencies in temporal graphs is evident in anomaly detection and predictive dynamic network analysis. This paper introduces a class of data dependencies called *Temporal Graph Functional Dependencies (TGFs)*. TGFs generalize functional dependencies to temporal graphs as a sequence of graph snapshots that are induced by time intervals, and enforce both topological constraints and attribute value dependencies that must be satisfied by these snapshots. (1) We establish the complexity results for the satisfiability and implication problems of TGFs. (2) We propose a sound and complete axiomatization system for TGFs. (3) We also present efficient parallel algorithms to detect inconsistencies in temporal graphs as violations of TGFs. The algorithm exploits data and temporal locality induced by time intervals, and uses incremental pattern matching and load balancing strategies to enable feasible error detection in large temporal graphs. Using real datasets, we experimentally verify that our algorithms achieve lower runtimes compared to existing baselines, while improving the accuracy over error detection using existing graph data constraints, e.g., GFDs and GTARs with 55% and 74% gain in F_1 -score, respectively.

Index Terms—temporal graph functional dependencies, graph data quality, temporal graphs

I. INTRODUCTION

Data constraints have been extended for graphs to capture inconsistencies and errors in graph data [1]–[3]. Given a graph G , a graph data dependency is often of the form of $(Q, X \rightarrow Y)$, where Q is a graph pattern that specifies a set of subgraphs in G via graph pattern matching (e.g., subgraph isomorphism) such that each subgraph should satisfy the value constraints enforced by $X \rightarrow Y$ (where X and Y are literals from the graph pattern). Notable examples include graph functional dependencies (GFDs) [1], graph keys (GKeys) [2] and graph association rules (GTARs) [4], [5].

Existing graph dependencies are often designed to capture inconsistencies in static graphs. Nevertheless, data errors also occur in *evolving* real-world graphs. In such scenarios, node attribute values and edges in graphs experience constant changes over time, and data consistency may persist only over a fraction of graphs specified by certain time periods. The need for modeling data consistency in temporal graphs that are time-dependent is evident in time sensitive applications such

as policy-making [6] and anomaly detection in health care [7], [8]. Data constraints for static graphs are often insufficient to satisfy such needs, as illustrated next.

Example 1: Consider a graph pattern Q (consisting of the solid, blue vertices) shown in Figure 1(a) describing patients with a specific disease are treated with an administered medication and dosage within a time interval. Figure 1(b) shows a temporal graph with matches of Q that monitors medicare activities [8]. A snapshot describes patient diagnosis, medication, and dosage taken at a timestamp. Federal drug regulating agencies, such as the Food and Drug Administration, receive numerous medication error reports due to missed doses, incorrect preparation and administration of drug formulations. To counter this, safe practice recommends that administered dosages be verified against patient characteristics, and require past and subsequent doses be correctly timed [9].

Figure 1(b) shows patients treated with medication *Veklury*, which requires if the intravenous (IV) infusion is between 30 to 120 mins, then the dosage must be 100mg [7]. At the current time $t_c = t_3$, continual validation of the dosage compares to past drug administrations (at least 30 but no more than 120 mins away) that must be 100mg (correct dosages indicated via green check marks). An incorrect dosage of 50mg is captured at t_6 . This time-sensitive rule can be expressed by posing a value constraint on the dosage to patients who match Q , *conditioned* by a time infusion period. To capture violations requires comparing a fraction of “snapshots” induced by a time period. Existing data constraints cannot express such consistency criteria for temporal graphs. \square

The above example calls for the need to model data consistency with respect to (w.r.t.) topological constraints and attribute values that are contextualized over a time interval duration. For each “current time” t_c , there is a need to compare matches at t_c against historical and future matches that are at least p but no more than q time units away. These “minimum” and “maximum” time bounds pose additional requirements where structural and literal conditions specified via graph pattern matching should hold.

Such schema and temporal constraints cannot be readily captured by prior graph dependencies and rules [1], [10], [11]. For example, GFDs cannot express the temporal constraints that perform necessary pairwise comparisons of single snap-

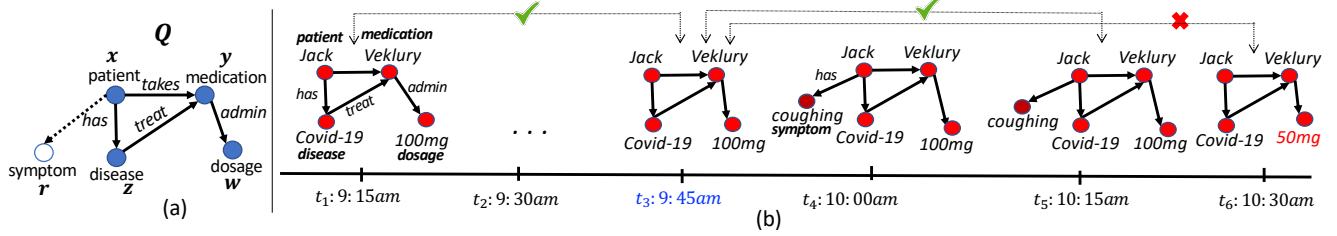


Fig. 1: Temporal data constraint to validate drug dosage at t_3 .

shots induced by minimum and maximum time ranges. Even if time periods were captured via graph attributes, modeling such semantics would involve an excessive number of GFDs, making them infeasible to be verified in practice. GTARs detects delayed co-occurrences of events via graph pattern matching, and do not model value dependencies [11]. We address the above challenges, and study several questions. (1) How to formalize such temporal data constraints in dynamic graphs? (2) What is the hardness of the fundamental problems (satisfiability, implication, validation) for these temporal data constraints? (3) How to efficiently detect violations with these dependencies in evolving graphs?

Contributions. We introduce Temporal Graph Functional Dependencies (TGFDs), a class of data dependencies to model the time-dependent consistency of temporal graph data, and study its fundamental problems and inconsistency detection.

(1) We introduce a formal model of TGFDs. TGFDs model time-dependent data consistency of temporal graphs by enforcing value dependencies that are conditioned by topological and temporal constraints in terms of temporal graph pattern matching. TGFDs apply conditionally to temporal graphs, and hold on graph snapshots that are induced by time intervals with lower and upper bounds. A special case of TGFDs with size-bounded graph patterns and their benefit in capturing data errors has been justified by our pilot study [12]. Providing a formal model for general TGFDs is our first contribution.

(2) We study the satisfiability, implication, and validation problems for TGFDs. We introduce an implication algorithm for TGFDs, and the notion of *temporal closure* that considers the time intervals of inferred values. We also develop a sound and complete TGFD axiom system for the implication of TGFDs (Section III).

(3) We introduce two TGFD-based inconsistency detection algorithms for temporal graphs: (i) an incremental detection algorithm (IncTED) that re-uses the matches and inconsistencies captured from earlier graph snapshots to compute updated matches and errors given graph changes; and (ii) a parallel algorithm (ParallelTED) that performs fine-grained estimations of the workload by computing the fraction of data induced by the literal conditions and the time interval duration in a TGFD. We show that these algorithms have time costs that are independent of the size of temporal graphs, and are feasible for large graphs (Section IV).

(4) We conduct an extensive evaluation over real data collections. We verify the efficiency of ParallelTED over a wide range of parameters achieving 120% and 29% speedup over sequential and GFD-based baselines, respectively, demonstrating TGFD error detection is feasible over real graphs. We show the effectiveness of ParallelTED over error detection using GFDs and GTARs with up to 55% and 74% gain in F_1 -score, respectively. Lastly, we conduct a case study with real examples of TGFDs, and the detected inconsistencies to demonstrate the utility of TGFDs in practice (Section V).

II. TEMPORAL GRAPH FUNCTIONAL DEPENDENCIES

We start with a notion of temporal graph pattern matching, and then introduce TGFD syntax and semantics.

A. Temporal Graph Pattern Matching

Temporal Graphs. We consider a temporal graph $\mathcal{G}_T = \{G_1, \dots, G_T\}$ as a sequence of graph snapshots. Each snapshot G_t ($t \in [1, T]$) is a graph (V, E_t, L_t, F_{A_t}) with a fixed node set V and edge set $E_t \subseteq V \times V$. Each node $v \in V$ (resp. edge $e \in E_t$) has a label $L_t(v)$ (resp. $L_t(e)$) at time t . For each node v , $F_{A_t}(v)$ is a tuple $(A_{1,t} = a_1, \dots, A_{n,t} = a_n)$ specifying a value of each attribute of v at time t .

Temporal graph pattern matching. A graph pattern is a directed, connected graph $Q[\bar{x}] = (V_Q, E_Q, L_Q, \mu)$ with a set of nodes V_Q and edges $E_Q \subseteq V_Q \times V_Q$. For each node $u \in V_Q$ and each edge $e \in E_Q$, the function L_Q assigns a label $L_Q(u)$ and $L_Q(e)$ to u and e , respectively. \bar{x} is a set of variables, and μ is a function that maps each $u \in V_Q$ to a distinct variable in \bar{x} . We shall refer to $\mu(u)$ as u for simplicity.

Matches. Given a temporal graph \mathcal{G}_T and pattern Q , a *match* $h_t(\bar{x})$ between a snapshot G_t of \mathcal{G}_T and pattern Q is a subgraph $G'_t = (V'_t, E'_t, L'_t, F'_{A_t})$ induced by V'_t of G_t that is isomorphic to Q . That is, there exists a bijective function (a matching) h_t from V_Q to V'_t such that: (1) for each node $u \in V_Q$, $L_Q(u) = L'_t(h_t(u))$; and (2) for each edge $e = (u, u') \in Q$, there is an edge $e' = (h_t(u), h_t(u'))$ in G'_t such that $L_Q(e) = L'_t(e')$. If $L_Q(u)$ is $'_'$, then it matches with any label for any timestamp t .

As a matching h_t uniquely determines a match (subgraph) for \bar{x} at any time t , we refer to a match as h_t for simplicity. Table I summarizes our notation and symbols.

TABLE I: Notations and symbols.

Symbol	Description
\mathcal{G}_T, G_t, G'_t	temporal graph, snapshot, and subgraph
$Q[\bar{x}]$	graph pattern
σ, Σ	a single TGFDF, and a set of TGFDFs
h_t	a match of $Q[\bar{x}]$ in G_t at time t
$\mathcal{E}(\mathcal{G}_T, \sigma), \mathcal{E}(\mathcal{G}_T, \Sigma)$	violations of σ, Σ in \mathcal{G}_T
$\mathcal{M}(Q, G_t)$	match set of Q in G_t
I_{h_i}, I_{h_j}	time domain of h_i, h_j
$\rho(i)$	permissible range of h_i
Π_X, π_{XY}	matches with shared values in X, XY
$\Gamma(\Pi_X)$	timesteps of matches in Π_X
$\mu_X(h_i)$	returns π_{XY} where h_i belongs

B. Temporal Graph Functional Dependencies

Syntax. A *Temporal Graph Functional Dependency* (TGFDF) σ is a triple $(Q[\bar{x}], \Delta, X \rightarrow Y)$, where:

- $Q[\bar{x}]$ is a graph pattern;
- $\Delta = (p, q)$ is a time interval, specified by a lower bound p , and an upper bound q (p, q are integers and $q \geq p \geq 0$);
- a value dependency $X \rightarrow Y$, where X and Y are two (possibly empty) sets of literals defined on \bar{x} .

Literals are of the form $u.A = c$ (constant literal) or $u.A = u'.A'$ (variable literal), where $u \in \bar{x}$, A and A' are attributes, and c is a constant. A TGFDF σ enforces three constraints:

- 1) topological and label constraint of pattern Q ,
- 2) a value dependency specified by $X \rightarrow Y$, and
- 3) a time interval constraint Δ , which specifies, for a time t , two time windows $[t - q, t - p]$ and $[t + p, t + q]$. The time windows induce the set of snapshots over which the constraint should hold (see ‘‘Semantics’’).

For simplicity, we consider *w.l.o.g.* TGFDFs in a normal form, *i.e.*, with a dependency $X \rightarrow Y$ where Y contains a single literal. We justify the normal form in Section III-C.

Example 2: We define a TGFDF $\sigma = (Q[\bar{x}], \Delta = (30, 120), [x.name, z.name = Covid19, y.name = Veklury] \rightarrow [w.val = 100mg])$. If a patient has *Covid-19* and is treated with *Veklury* over IV infused between 30 to 120 mins, then the dosage is *100mg*. \square

Semantics. Given a temporal graph \mathcal{G}_T , a TGFDF enforces value dependencies between any pair of snapshots that are (1) matches via graph pattern matching, and (2) having timestamps within time ranges in Δ , for any timestamp in $[1, T]$. Consider a TGFDF $\sigma = (Q[\bar{x}], \Delta, X \rightarrow Y)$, and a pair of matches (h_i, h_j) of Q in G_i and G_j , respectively ($i, j \in [1, T]$). We say (h_i, h_j) *matches* σ if

- (h_i, h_j) satisfies X (denoted as $(h_i, h_j) \models X$), *i.e.*, for each constant literal $l = (u.A = c)$ (resp. variable literal $u.A = u'.A'$) in X , $h_i(u) = h_j(u) = c$ (resp. $h_i(u) = h_j(u')$); and
- $|j - i| \in \Delta$.

The term $|j - i| \in \Delta$ conveniently express temporal semantics including ‘‘future’’ and ‘‘past’’ from their conventional counterparts in temporal integrity constraints [13] to temporal

graphs. For any specific timestamp $i \in [1, T]$, (a) if $i \leq j$, then $|j - i| \in \Delta$ specifies any timestamp j from a ‘‘future’’ time window $[i + p, i + q]$; (b) if $i > j$, then $|j - i| \in \Delta$ specifies timestamps j from a ‘‘past’’ time window $[i - q, i - p]$. Given a time interval Δ , a TGFDF σ enforces data consistency over all pairs $(h_i, h_j) \in [1, T]$ that matches σ in terms of Δ .

For any pair (h_i, h_j) that does not match σ , (h_i, h_j) ‘‘trivially’’ satisfies σ . We say a temporal graph \mathcal{G}_T *nontrivially satisfies* a TGFDF σ , denoted as $\mathcal{G}_T \models \sigma$, if (a) there exists at least a pair of matches (h_i, h_j) that also matches σ , and (b) $(h_i, h_j) \models \sigma$. \mathcal{G}_T satisfies a set of TGFDFs Σ if for every $\sigma \in \Sigma$, $\mathcal{G}_T \models \sigma$.

Example 3: Figure 1(b) shows matches (h_1, h_3) and (h_3, h_5) satisfy σ (denoted with a green check mark), but $(h_3, h_6) \not\models \sigma$, having the wrong dosage of *50mg* at t_6 (denoted with a red x) given the required infusion time of 30 to 120 minutes. \square

Remarks. As justified in our pilot study [12] on a special case of the general TGFDFs with bounded pattern size over a real knowledge graph DBpedia, we found over 140 temporal data constraints in real knowledge base DBpedia. Of these constraints, 28% can capture at least one inconsistency; and each constraint can capture on average 7 distinct erroneous attribute values that span over 5 timesteps.

Relationship to Other Dependencies. GFDs define topological and attribute dependence over *static* graphs. TGFDFs subsume GFDs as a special case when $\Delta = (0, 0)$. GTARs are soft rules that use an approximate subgraph isomorphism matching, only consider matching with time intervals $p = 0$, and do not include historical matches as part of their semantics.

III. FOUNDATIONS

We next study the satisfiability, implication and validation problems for TGFDFs, and present an axiomatization.

A. Satisfiability

A set Σ of TGFDFs is *satisfiable*, if there exists a temporal graph \mathcal{G}_T , such that $\mathcal{G}_T \models \Sigma$. The satisfiability problem is to determine whether Σ is satisfiable. Satisfiability checking helps to decide whether a set of TGFDFs Σ are ‘‘inconsistent’’ before being applied for error detection in temporal graphs.

Example 4: Define pattern Q' by augmenting Q with an edge from *patient* (x) to *symptom* (r) (shown as a dotted edge in Figure 1(a)). Consider σ' defined over Q' as $\sigma' = (Q'[\bar{x}], \Delta = (30, 120), [x.name, r.name, z.name = Covid19, y.name = Veklury] \rightarrow [w.val = 20mL])$, with $Q \subseteq Q'$. The consequent literal requires the value of w to be equal to *100mg* and *20mL* simultaneously, leading to ‘‘conflicting’’ value constraints. Since any match of σ will also match σ' , there is no temporal graph \mathcal{G}_T that satisfies both. Thus, $\{\sigma, \sigma'\}$ are not satisfiable. \square

The ‘‘conflicting’’ value constraints do not necessarily lead to unsatisfiable TGFDFs. In the above example, suppose the Δ time interval durations for σ, σ' were $(30, 120)$ and

(20, 25), respectively, then one can verify that they do become satisfiable as the time intervals are not overlapping. This requires computing the time intervals of when derived values and literals are expected to hold. This illustrates that TGF D satisfiability analysis is more involved than GFDs: the “conflicting” value constraints are conditioned upon both *pattern matching and the temporal constraints*. To characterize this, we introduce a notion of TGF Ds *embeddings*. The notion has its foundation in [1], and is extended for TGF Ds with temporal constraints.

Pattern embedding [1]. We say a graph pattern $Q'[\bar{x}'] = (V'_Q, E'_Q, L'_Q, \mu')$ is *embeddable* in another pattern $Q[\bar{x}] = (V_Q, E_Q, L_Q, \mu)$, if there exists a mapping f from V'_Q to a subset of nodes in V_Q that preserves node labels of V'_Q , all the edges induced by V'_Q and corresponding edge labels. Moreover, f induces a “renaming” of each variable $x \in \bar{x}$ to a distinct variable x' in \bar{x}' , i.e., for each variable $x \in \bar{x}$, $\mu'(f(\mu^{-1}(x))) = x' \in \bar{x}'$.

TGF Ds Embedding. Given two TGF Ds $\sigma = (Q[\bar{x}], \Delta, f(X') \rightarrow f(Y'))$ and $\sigma' = (Q'[\bar{x}'], \Delta', X' \rightarrow Y')$, We say that σ is a (temporally) *overlapped* TGF D of σ' w.r.t. graph pattern Q , if (1) Q' is embeddable in Q , and (2) $(\Delta \cap \Delta') \neq \emptyset$. Moreover, σ is a (temporally) *embedded* TGF D of σ' w.r.t. Q if $\Delta' \subseteq \Delta$. Given a set of TGF Ds Σ and a graph pattern Q , we denote as Σ_Q (resp. $\Sigma_{Q, \{\Delta, \Delta'\}}$) the set of embedded (resp. overlapped TGF Ds) w.r.t. Q .

Example 5: In Figure 1(a), Q is an embedded pattern in Q' as there exists a subgraph isomorphism mapping from Q to a subgraph of Q' . Moreover, consider a TGF D σ'' with $\Delta'' = (20, 60)$, then σ'' is a (temporally) overlapped TGF D of σ . Lastly, σ is a (temporally) embedded TGF D of σ' . \square

In contrast to GFDs, TGF D satisfiability requires checking whether conflicting literal values occur during overlapping time intervals, leading to non-satisfiability. This requires us to consider the notion of *temporal closure* for TGF Ds.

Definition 3.1: (Temporal Closure) Given a set of overlapped TGF Ds $\Sigma_{Q, \{\Delta, \Delta'\}}$ w.r.t. a graph pattern Q , the *temporal closure* of a set $\Sigma_{Q, \{\Delta, \Delta'\}}$, denoted as $\text{closure}(X, \Sigma_{Q, \{\Delta, \Delta'\}})$, refers to the set of literals that are derivable via transitivity of equality atoms in X over $\Sigma_{Q, \{\Delta, \Delta'\}}$. The temporal closure of a set of TGF Ds Σ (denoted as $\text{closure}(\Sigma)$), refers to all the literals $\text{closure}(X, \Sigma_{Q, \{\Delta, \Delta'\}})$ with Q ranging over the patterns from the TGF Ds in Σ . \square

We outline an algorithm below to compute $\text{closure}(\Sigma)$. First, given a set of TGF Ds Σ , it first adds all Y seen in a TGF D $\sigma \in \Sigma$, if $(Q[\bar{x}], \delta, \emptyset \rightarrow Y) \in \Sigma$. Second, for each pattern Q seen in Σ , it then computes the overlapped TGF Ds $\Sigma_{Q, \{\Delta, \Delta'\}}$. For each literal Y seen in $X \rightarrow Y$ in a TGF D $\sigma \in \Sigma_{Q, \{\Delta, \Delta'\}}$, if $X \subseteq \text{closure}(\Sigma)$ or can be derived via transitivity of equality atoms in $\text{closure}(\Sigma)$, then it adds Y to $\text{closure}(\Sigma)$. For example, if $x.A = u$ and $y.B = u$ are in $\text{closure}(\Sigma)$, then $x.A = y.B$ can be derived and added to

$\text{closure}(\Sigma)$. This will give us the set of literals that are to be enforced in $\Sigma_{Q, \{\Delta, \Delta'\}}$.

For each derived value, we compute the time intervals over which each literal value is expected to hold. We say $\text{closure}(X, \Sigma_{Q, \{\Delta, \Delta'\}})$ is *in conflict*, if $\text{closure}(X, \Sigma_{Q, \{\Delta, \Delta'\}})$ contains literals $x.A = a$ and $y.B = b$, and $a \neq b$. Given Σ , the temporal closure $\text{closure}(\Sigma)$ is in conflict, if there exists a pattern Q from a $\sigma \in \Sigma$ such that $\text{closure}(X, \Sigma_{Q, \{\Delta, \Delta'\}})$ is in conflict. We show the following result.

Lemma 1: A set Σ of TGF Ds is not satisfiable if and only if $\text{closure}(\Sigma)$ is in conflict. \square

The result below verifies that checking TGF D satisfiability is not harder than their GFD counterparts. For brevity, all proofs in this section are in the extended version [14].

Theorem 1: The satisfiability problem for TGF Ds is coNP-complete. \square

Proof sketch: We introduce an NP algorithm for checking the complement of TGF D satisfiability, which is to decide if a given set of TGF Ds Σ is not satisfiable. Based on Lemma 1, the algorithm guesses (1) a graph pattern Q seen in Σ , (2) a subset $\Sigma' \subseteq \Sigma$, (3) a subgraph isomorphism mapping from each pattern Q' seen in Σ' to Q . It then verifies if Σ' is a set of overlapped TGF Ds w.r.t. Q , by verifying, for each pair of TGF Ds $\sigma_1, \sigma_2 \in \Sigma'$ with time intervals Δ_1 and Δ_2 , (a) whether their respective patterns Q_1, Q_2 are isomorphic to a subgraph in Q , and (b) whether the time intervals $(\Delta_1 \cap \Delta_2) \neq \emptyset$. If so, It then invokes the aforementioned algorithm to check if the temporal closure $\text{closure}(X, \Sigma_{Q, \{\Delta, \Delta'\}})$ is in conflict. If so, it returns “yes” (Σ is not satisfiable). The above process is in NP given bounded number of pairwise verification and conflict checking in PTIME.

The lower bound is verified by a reduction from GFD satisfiability with constant literals [1]. A TGF D counterpart can be constructed by introducing, for each GFD, a time interval $[0, 0]$, and a temporal graph with a single snapshot. As GFD satisfiability with constant literals is already coNP-hard, the lower bound follows. \square

B. Implication

Given a set of TGF Ds Σ and a $\sigma \notin \Sigma$, we say Σ implies σ , denoted $\Sigma \models \sigma$, if for any \mathcal{G}_T , if $\mathcal{G}_T \models \Sigma$, then $\mathcal{G}_T \models \sigma$. If $\Sigma \models \sigma$, then σ is a logical consequence of Σ . Given Σ and σ , the implication problem is to determine whether $\Sigma \models \sigma$. Implication analysis helps us to remove redundant TGF Ds and perform error detection with a smaller number of rules.

To check whether $\Sigma \models \sigma$, we extend the temporal closure in Section III-A to a counterpart for embedded TGF D set Σ_Q (denoted as $\text{closure}(X, \Sigma_Q)$). The temporal closure $\text{closure}(X, \Sigma_Q)$ is a set of pairs (Y, Δ) , where Y is a literal, and Δ is an associated time interval called the *validity period* in which Y should hold. We outline a new algorithm that

computes $\text{closure}(X, \Sigma_Q)$. In contrast to GFD implication, we must compute the sub-intervals on which derived literals are expected to hold after applying each TGF. The increased space of literals is managed by indexing literals, and searching for overlapping time intervals at each apply step.

- (i) **Initialize:** for each literal $x \in X$, add (x, Δ) to $\text{closure}(X, \Sigma_Q)$.
- (ii) **Apply:** for each $\sigma' \in \Sigma_Q$, where $\sigma' = (Q'[\bar{x}], \Delta', X' \rightarrow Y')$, if all literals $x' \in X'$ can be derived via transitivity of equality of values from the literals in $\text{closure}(X, \Sigma_Q)$, then add $(Y', \Delta' \cap \Delta'')$ to $\text{closure}(X, \Sigma_Q)$.
- (iii) **Merge:** for a literal Y'' and all $\{(Y'', \Delta''_1), \dots, (Y'', \Delta''_m)\}$ in the $\text{closure}(X, \Sigma_Q)$, merge the time intervals and replace the pairs with a single pair $(Y'', (\Delta''_1 \cup \dots \cup \Delta''_m))$.

The above process is in PTIME. We say a literal Y is *deducible* from Σ and X , if there exists a Σ_Q derived from Σ , and a pair $(Y, \Delta'') \in \text{closure}(X, \Sigma_Q)$ such that $\Delta \subseteq \Delta''$.

Lemma 2: *Given a set of TGFs Σ and a TGF $\sigma = (Q(\bar{x}), \Delta, X \rightarrow Y)$, $\Sigma \models \sigma$ if and only if Y is deducible from Σ and X .* \square

Theorem 2: *The implication problem for TGFs is NP-complete.* \square

Proof sketch: We provide an NP algorithm that, given Σ and $\sigma = (Q(\bar{x}), \Delta, X \rightarrow Y)$, guesses a subset Σ' of Σ , and a mapping from the patterns of each TGF in Σ' to the pattern of σ , to verify if Σ' is the embeddable set of TGFs in Σ_Q . If so, it invokes the aforementioned procedure to compute the temporal closure of Σ_Q , and verify if Y is deducible. Specifically, it checks the validity period of the enforced literals during the Apply step, i.e., checking whether $(\Delta' \cap \Delta'') \neq \emptyset$ for time intervals Δ', Δ'' from $\sigma' \in \Sigma_Q$, and literal (Y'', Δ'') , respectively. The verification is in PTIME for a finite number of literals in the closure and $|\Sigma_Q|$. For the lower bound, the implication of TGF is NP-hard by reduction from the implication of GFDs, which is known to be NP-complete [1]. \square

C. Axiomatization

We present an axiomatization for TGFs. The first five axioms also apply to GFDs (no axioms were defined for GFDs [1]). Our axiomatization is sound and complete [14].

Axiom 1: (Literal Reflexivity) *For a given $Q[\bar{x}]$, X, Y are sets of literals, if $Y \subseteq X$, then $X \rightarrow Y$.* \square

In Axiom 1, a set of literals Y that is a subset of literals X , will induce a trivial dependency $X \rightarrow Y$ for any Δ .

Axiom 2: (Literal Augmentation) *If $\sigma' = (Q[\bar{x}], \Delta, X' \rightarrow Y)$, $\sigma = (Q[\bar{x}], \Delta, X \rightarrow Y)$, and $X' \subseteq X$, then $\sigma' \models \sigma$.* \square

If $X' \rightarrow Y$ holds, then literals in X', Y are in $\text{closure}(X, \Sigma_Q)$. Since $X' \subseteq X$, we can derive Y , and σ holds.

Axiom 3: (Pattern Augmentation) *If $\sigma' = (Q'[\bar{x}], \Delta, X \rightarrow Y)$, and $\sigma = (Q[\bar{x}], \Delta, X \rightarrow Y)$, $Q' \subseteq Q$, then $\sigma' \models \sigma$.* \square

In Axiom 3, if Q' is isomorphic to a subgraph of Q , and if σ' (with pattern Q') holds, it will continue to hold under Q .

Axiom 4: (Transitivity) *If $\sigma' = (Q'[\bar{x}], \Delta, X \rightarrow W)$, $\sigma = (Q[\bar{x}], \Delta, W \rightarrow Y)$, where $Q' \subseteq Q$, then for any $\sigma'' = (Q[\bar{x}], \Delta, X \rightarrow Y)$, it follows that $\{\sigma, \sigma'\} \models \sigma''$.* \square

In Axiom 4, all matches that satisfy σ' will also be contained within matches satisfying σ since $Q' \subseteq Q$. By transitivity of equality w.r.t. the literals in W , these matches of Q will satisfy $X \rightarrow Y$, thereby showing $\{\sigma, \sigma'\} \models \sigma''$.

Axiom 5: (Decomposition) *If $\sigma = (Q[\bar{x}], \Delta, X \rightarrow Y)$ with $Y = \{l_1, l_2\}$, then for $\sigma' = (Q[\bar{x}], \Delta, X \rightarrow l_1)$ and $\sigma'' = (Q[\bar{x}], \Delta, X \rightarrow l_2)$, it follows that $\sigma \models \{\sigma', \sigma''\}$.* \square

Verifying the literals in Y can be done simultaneously in one verification (via σ), or in conjunction (via σ', σ'').

Axiom 6: (Interval Intersection) *If $\sigma = (Q[\bar{x}], (p, q), X \rightarrow Y)$, $\sigma' = (Q[\bar{x}], (p', q'), X \rightarrow Y)$, then for $\sigma'' = (Q[\bar{x}], (p'', q''), X \rightarrow Y)$, where $(p'', q'') = (p, q) \cap (p', q')$, it follows that $\{\sigma, \sigma'\} \models \sigma''$.* \square

For σ, σ' with matches satisfying $X \rightarrow Y$ over Δ, Δ' , respectively, requires verifying all pairwise matches over all sub-intervals $\Delta'' \subseteq (\Delta \cap \Delta')$, thereby showing $\{\sigma, \sigma'\} \models \sigma''$.

Axiom 7: (Interval Containment) *If $\sigma = (Q[\bar{x}], \Delta, X \rightarrow Y)$, and $\sigma' = (Q[\bar{x}], \Delta', X \rightarrow Y)$, $\Delta' \subseteq \Delta$, then $\sigma \models \sigma'$.* \square

If σ holds over Δ , then it will hold over any subsumed Δ' that is more restrictive. Pairwise matches over all sub-intervals $\Delta' \subseteq \Delta$ must also satisfy the dependency, thus σ' holds.

Theorem 3: *The axiomatization is sound and complete.* \square

Proof: Axioms 1-5 are sound as described above. To show completeness of Axioms 1-4, recall that the $\text{closure}(X, \Sigma_Q)$ is defined over all embedded TGFs for a pattern Q , i.e., by Axiom 3, if σ' holds over $Q' \subseteq Q$, then σ holds for pattern Q . In computing $\text{closure}(X, \Sigma_Q)$, inference of valid time intervals is done by checking Axiom 6, where the interval overlap is non-empty. For $\sigma = (Q[\bar{x}], \Delta, X \rightarrow y)$ can be inferred from Σ , if and only if there exists a literal $(y, \Delta'') \in \text{closure}(X, \Sigma_Q)$ such that $\Delta \subseteq \Delta''$.

To show completeness, it is sufficient to show that for any σ , if $\Sigma \not\models \sigma$, then there exists a \mathcal{G}_T such that $\mathcal{G}_T \models \Sigma$, but $\mathcal{G}_T \not\models \sigma$, i.e., Σ does not logically imply σ . First, we show that $\mathcal{G}_T \models \sigma'$, for all $\sigma' \in \Sigma$, and then show σ is not satisfied by \mathcal{G}_T . Suppose $\sigma' = (Q[\bar{x}], \Delta, V \rightarrow W)$ is in Σ but not satisfied by \mathcal{G}_T . Then $(V, \Delta) \in \text{closure}(X, \Sigma_Q)$, and (W, Δ) nor any subset of literals of W can be in $\text{closure}(X, \Sigma_Q)$, otherwise, σ' would be satisfied by \mathcal{G}_T . Let (w, Δ) be a literal of W

not in $\text{closure}(X, \Sigma_Q)$. We have $\sigma'' = (Q'[\bar{x}], \Delta, X \rightarrow V)$, since V is in the closure, and by Axiom 3 and Axiom 4, we have $\sigma''' = (Q[\bar{x}], \Delta, X \rightarrow W)$. By Axiom 1, we can infer $W \rightarrow w$ over the interval Δ , and by transitivity w.r.t. W over pattern Q , we have $X \rightarrow w$, which implies that $(w, \Delta) \in \text{closure}(X, \Sigma_Q)$, which is a contradiction. Hence, $\mathcal{G}_T \models \Sigma$, for all $\sigma' \in \Sigma$. Second, we show that for a σ , if $\Sigma \not\models \sigma$, then $\mathcal{G}_T \not\models \sigma$. Let's suppose $\mathcal{G}_T \models \sigma$, then $(y, \Delta) \in \text{closure}(X, \Sigma_Q)$. However, if this is true, then $\Sigma \models \sigma$, which is a contradiction. Hence, $\mathcal{G}_T \not\models \sigma$, and the axiomatization is complete.

D. Validation

Given Σ , and a temporal graph \mathcal{G}_T , the validation problem is to decide whether $\mathcal{G}_T \models \Sigma$. A practical application of validation is to detect *violations* of Σ in \mathcal{G}_T . We say a pair of matches (h_i, h_j) is a violation (“error”) of a TGF D $\sigma = (Q(\bar{x}), \Delta, X \rightarrow Y) \in \Sigma$, if (h_i, h_j) matches σ and $(h_i, h_j) \not\models Y$. We denote the set of violations of Σ in \mathcal{G}_T as $\mathcal{E}(\mathcal{G}_T, \Sigma)$. The validation problem is to decide whether $\mathcal{E}(\mathcal{G}_T, \Sigma)$ is empty.

Theorem 4: *The validation of TGF Ds is coNP-complete.* \square

Proof sketch: The lower bound can be verified from the GFDs counterpart, where the validation problem is coNP-complete [1]. For TGF Ds, an NP algorithm returns “yes” if $\mathcal{G}_T \models \Sigma$ as follows. It (1) guesses a TGF D σ , and guesses and verifies a pair of mappings $(h_{t_i}(\bar{x}), h_{t_j}(\bar{x}))$ over a finite number of sub-intervals $\{[t_i, t_j] \mid 1 \leq i, j \leq T, |t_j - t_i| \in \Delta\}$, and (2) checks whether $(h_{t_i}(\bar{x}), h_{t_j}(\bar{x})) \models X$, but $(h_{t_i}(\bar{x}), h_{t_j}(\bar{x})) \not\models y$, if so, return “yes”. Checking all matches over the intervals is in PTIME. Since the complement to the decision problem still remains in NP, the validation problem for TGF Ds is coNP-complete, no harder than its GFDs counterpart. \square

IV. PARALLEL TGF D ERROR DETECTION

We introduce a parallel TGF D error detection algorithm, ParallelTED, that includes fine-grained workload estimation, temporal pattern matching with match maintenance over evolving graph fragments, and incremental error detection that avoids all pairwise match enumerations.

A Sequential Algorithm. Given a TGF D $\sigma = (Q(\bar{x}), \Delta, X \rightarrow Y)$, a sequential algorithm computes $\mathcal{E}(\mathcal{G}_T, \Sigma)$ as follows. (1) For each snapshot $G_t \in \mathcal{G}_T$, it computes from scratch all matches of Q in G_t , and those in the subsequent snapshots G_j where $|j - t| \in \Delta$ (if not computed yet). (2) It then verifies, for each pair of matches of Q $\{(h_i, h_j)\}$ with $|j - i| \in \Delta$, if $(h_i, h_j) \models X$ (i.e., (h_i, h_j) matches σ), and $(h_i, h_j) \not\models Y$. If so, a violation (h_i, h_j) is identified and added to $\mathcal{E}(\mathcal{G}_T, \Sigma)$. This approach separately performs pattern matching and TGF D validation, and is infeasible for large graphs due to an excessive number of subgraph isomorphism tests (which is known to be NP-complete [15]), and comparisons over each pairs of snapshots. As most changes in

real-world temporal graphs affect a small portion (e.g., 5-10% of nodes weekly [16]) and 80-99% of the changes are highly localized [17], this naturally motivates incremental and parallel solutions for TGF D-based error detection.

We next present ParallelTED, a *Parallel TGF D Error Detection* algorithm, for error detection in large \mathcal{G}_T . The algorithm fully exploits the temporal interval constraints to interleave parallel pattern matching and incremental error detection, in at most T rounds of parallel computation.

Overview. The algorithm ParallelTED (Algorithm 1) works with a set of n worker machines $M_1 \dots M_n$ and a coordinator M_c . It executes in total T supersteps. Each superstep t processes a *fragmentation* of a snapshot G_t as a set of subgraphs $\{F_{tr}\}$ of G_t ($t \in [1, T]$ and $r \in [1, n]$). Intuitively, we perform parallel computation to detect and maintain the set of violations $(\mathcal{E}(\{G_1, \dots, G_t\}, \Sigma))$ over “currently observed” snapshots $\{G_1, \dots, G_t\}$, at each superstep t . The algorithm terminates after T supersteps, and ensures the correct computation of $\mathcal{E}(\mathcal{G}_T, \Sigma)$ given the correct update of violation set at each superstep.

Algorithm. ParallelTED maintains the following structures that are dynamically updated. (1) Each worker M_r maintains (a) a set of local matches of Q of snapshot G_t $M_r(Q, G_t)$, (b) a set of local violations $\mathcal{E}_r(\mathcal{G}_T, \Sigma)$, by only accessing local graphs (initialized as fragment $\{F_{tr}\}$), and (c) a set of “cross-worker” violations $\mathcal{E}_r(\mathcal{G}_T, \Sigma)$, which requires the comparison of two matches from M_r and a different worker. The coordinator maintains a set of global violations $\mathcal{E}(\mathcal{G}_T, \Sigma)$ to be assembled from local violations.

ParallelTED first invokes a procedure GenAssign to initialize and assigns a set of joblets (a set of lightweight validation tasks; see Section IV-A) to all the workers, and initializes global structures for incremental maintenance of the pattern matches (see Section IV-B) (lines 1-2). This cold-starts the parallel error detection upon the processing of the first fragmented snapshot in \mathcal{G}_T . It then runs in T supersteps in parallel (lines 3-10), following a bulk synchronous model, and processes one fragmented snapshot a time.

In each superstep t , each M_r executes the following two steps in parallel (lines 4-7): (1) incrementally updates a set of local matches $M_r(Q, G_t)$ and violations $\mathcal{E}_r(\mathcal{G}_T, \Sigma)$ over fragmented snapshot $\{F_{tr}\}$ by invoking LocalVio (line 4); and (2) requests a small amount of edges from other workers, and invokes IncTED to incrementally detect the violations $\mathcal{E}_c(\mathcal{G}_T, \Sigma)$ across two workers (line 5; see Section IV-B). M_r then returns the updated local violations (augmented with cross-worker violations) to M_c (lines 6-7). The coordinator M_c incrementally maintains a set of global violations upon receiving the updated local violations (line 8), and invokes GenAssign to rebalance the workload for the next superstep (lines 9-10) upon a triggering condition. This validates Σ over the snapshots $\{G_1, \dots, G_t\}$ “seen” thus far.

Algorithm 1: ParallelTED (\mathcal{G}_T, Σ)

```
1 Initialize  $\Pi_X, \pi_{XY}, \Gamma(\Pi_X), \Gamma(\pi_{XY});$   
2 GenAssign ( $\mathcal{G}_T, \Sigma$ );  
3 foreach  $t \in T$  do  
   /* at worker  $r$  in parallel */  
4    $\mathcal{E}_r(F_r, \Sigma) := \mathcal{E}_r(F_r, \Sigma) \cup \text{LocalVio}(F_{tr}, \mathcal{J}_{tr}, t);$   
5    $\mathcal{E}_c(\mathcal{G}_T, \Sigma) := \mathcal{E}_c(\mathcal{G}_T, \Sigma) \cup \text{IncTED}(G_t, \Sigma,$   
    $\mathcal{M}_r(Q, G_t));$   
6    $\mathcal{E}_r(F_r, \Sigma) := \mathcal{E}_r(F_r, \Sigma) \cup \mathcal{E}_c(\mathcal{G}_T, \Sigma);$   
7   return  $\mathcal{E}_r(F_r, \Sigma);$   
   /* at the coordinator side */  
8    $\mathcal{E}(\mathcal{G}_T, \Sigma) := \mathcal{E}_c(\mathcal{G}_T, \Sigma) \cup \bigcup_r \mathcal{E}_r(F_r, \Sigma);$   
9   if  $(t_{\mathcal{J}_{tr}} < ((1 - \zeta) \cdot t_l)) \vee (t_{\mathcal{J}_{tr}} > ((1 + \zeta) \cdot t_u))$  then  
10  | Assign ( $\mathcal{J}_{tr}, CCost$ ); /* rebalance workload */  
11 return  $\mathcal{E}(\mathcal{G}_T, \Sigma);$ 
```

Procedure GenAssign (\mathcal{G}_T, Σ)

/* at the coordinator side */

```
1  $\mathcal{E}(\mathcal{G}_T, \Sigma) := \emptyset; \mathcal{E}_c(\mathcal{G}_T, \Sigma) := \emptyset; CCost := \emptyset;$   
2 foreach  $\sigma \in \Sigma$  do  
3 | Define  $\mathcal{J}_{tr}(\sigma, F_{tr}, \mathcal{G}_T)$  and estimate  $|\mathcal{J}_{tr}|;$   
4 | Estimate communication cost  $CCost(\mathcal{J}_{tr})$   
5 Assign ( $\mathcal{J}_{tr}, CCost$ );  
6 Send  $\mathcal{J}_{tr}$  across workers  $M_r$ ;
```

Optimizations. To cope with skewed localized updates that lead to stragglers and reduce communication overhead, ParallelTED adopts two strategies below.

(1) An adaptive time-interval aware workload balancing strategy (procedure GenAssign; line 6) to automatically (re-)partition the TGFD validation workload to maximize parallelism. The idea is to decompose validation tasks to a set of highly parallelizable, small subtasks that are induced by path patterns, time-intervals, and common literals (“Joblets”), and dynamically estimates a bounded subgraph induced by the joblets to be assigned and executed in parallel.

(2) ParallelTED also adopts an incremental pattern matching scheme (Algorithm IncTED; line 5) to maintain the local violations. The strategy performs case analysis of edge updates and only processes a necessary amount of validation, to reduce the communication and local detection cost. We next introduce the details of GenAssign and IncTED.

A. Time interval-Aware Workload Balancing

Large, evolving graphs pose additional efficiency challenges over static graphs, where delta changes between snapshots need to be incorporated.

Given a set of TGFDs Σ and \mathcal{G}_T , procedure GenAssign creates a set of “joblets” and estimates their processing cost for balanced workload assignment (as illustrated in Algorithm 1).

Joblets and Jobs. A *joblet* characterizes a small TGFD validation task that can be conducted by a worker in parallel. A joblet at superstep t is a triple $\omega_{trk}(Q_k, F_{tr}, \mathcal{G}(v', d))$, where

- $Q_k(v_k, d)$ is a sub-pattern of a pattern Q with a designated center node v_k and a radius d w.r.t. v_k , for a TGFD $\sigma = (Q[\bar{x}], \Delta, X \rightarrow Y)$ in Σ ;
- F_{tr} is a fragment of snapshot G_t on worker M_r ; and
- $\mathcal{G}(v', d) = \bigcup_{s, s' \leq t} \{\{G_s(v', d), G'_s(v', d)\} \mid |s' - s| \in \Delta\}$, where v and v' have the same label, and $G'_s(v', r)$ is a subgraph of G_s induced by v' and its d -hop neighbors.

Intuitively, a joblet encodes a fraction of a validation task to identify violations of a TGFD $\sigma \in \Sigma$. It is dynamically induced by incorporating a small fragment of Q and only the relevant fraction of snapshots in \mathcal{G}_T that should be checked to detect violations of σ with pattern Q and time interval Δ .

A *job* $\mathcal{J}_{tr}(\sigma, F_{tr}, \mathcal{G}_T)$ refers to a set of joblets that encode the workload to validate a TGFD σ with pattern Q . A job contains all joblets for all subqueries Q_k from Q . We denote as $\mathcal{J}_{tr}(\Sigma, F_{tr}, \mathcal{G}_T)$ the jobs for validating a set of TGFDs Σ , i.e., $\mathcal{J}_{tr}(\Sigma, F_{tr}, \mathcal{G}_T) = \bigcup_{\sigma \in \Sigma} \mathcal{J}_{tr}(\sigma, F_{tr}, \mathcal{G}_T)$.

We next introduce a path decomposition strategy adopted by GenAssign. The joblets are created accordingly for a given decomposition of $Q = \{Q_1, \dots, Q_K\}$.

K -Path decomposition (not shown in Algorithm 1). It has been shown that the cost of graph query processing can be effectively estimated using path queries [18]. GenAssign adopts a K -path pattern decomposition strategy for joblet creation and cost estimation. For each $\sigma \in \Sigma$, GenAssign decompose a pattern Q into a set of paths $\{Q_1, \dots, Q_K\}$, such that Q is the union of Q_k ($k \in [1, K]$). Each Q_k is a maximal path from a node v_{k_1} to a destination node v_{k_m} that cannot be further extended by pattern edges. Each Q_k is augmented with value constraints posed by the literals from $X \cup Y$.

Let v_k be a center node with minimum radius in each path pattern Q_k ($k \in [1, K]$), where the radius d is the longest shortest path between v_k and any node in Q_k . The joblets are then created with K -path decomposition and induced subgraphs w.r.t. v_k and Q_k ($k \in [1, K]$) accordingly. Figure 2(a) shows two (maximal) pattern paths Q'_1 and Q'_2 of the pattern Q' with the literal set $\{z = \text{McMaster}\}$.

Workload Estimation (line 4 of Procedure GenAssign). The workload is estimated as the size of joblets/jobs, and the expected communication cost among the workers. To estimate the joblet size, we adapt the cardinality estimation for graph queries [18]. We compute a probability distribution of the expected number of matches for each edge (v_l, v_{l+1}) in Q_k with label a_l . The distribution provides a probabilistic estimation of the number of matches of v_{l+1} , given the matches of v_l that are connected via an edge with label a_l and satisfy the literals over v_l and v_{l+1} . We estimate using the mean and standard deviation of the number of matches of v_{l+1} w.r.t. v_l . We compute the distribution function of Q_k as the product of the distribution functions of each consecutive edge in Q_k . We estimate the size of a job $|\mathcal{J}_{tr}(\sigma, F_{tr}, \mathcal{G}_T)|$ as the cardinality of the pattern Q , i.e., the number of matches of Q , computed

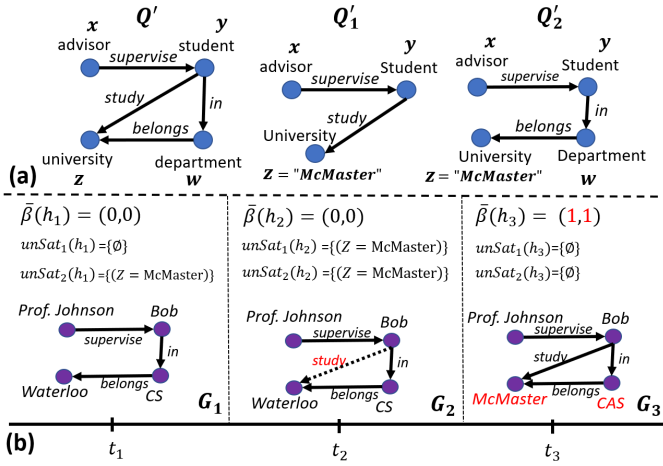


Fig. 2: Pattern paths and partial matches.

as the upper-bound of the minimum cardinality of all Q_k .

Communication cost estimation (line 10 of Algorithm ParallelTED; line 4 of ProcedureGenAssign). For a joblet $\omega_{trk}(Q_k, F_{tr}, \mathcal{G}(v', d))$, fragment F_{tr} may contain a partial match of a path Q_k , i.e., some nodes and edges that match Q_k reside in machine $M_{r'}, r' \neq r$. We must exchange these small number of edges between workers that we estimate as the communication cost of a joblet, defined as $CCost(\omega_{trk}) = \sum_{\substack{(v_1, v_2) \in G_t(v', d) \\ \neg((v_1, v_2) \in F_{tr})}} |(v_1, v_2)|$.

We aggregate over all the joblets containing pattern paths Q_k of Q to define the communication cost of a job, $CCost(\mathcal{J}_{tr}) = \sum_k CCost(\omega_{trk})$.

Workload Assignment and Rebalancing (lines 9-10 of ParallelTED; line 5 of GenAssign). We distribute jobs to workers such that the communication cost C , and the makespan τ is minimized. We solve a *general assignment (GA) problem* [19]. Given C and τ , the GA problem is to find an assignment of each job such that the total parallel cost is bounded by C , and minimizes the makespan. Following [19], we develop a pseudo-polynomial-time, 2-approximation algorithm. It performs a bisection search on the range of estimated makespan and keeps assignments with an objective function value less than half of the current best solution. It solves a linear program at most $\log(wP)$ times (w is the number of jobs and P is the job with maximum estimated workload) and selects the one with the smallest makespan. We introduce the details in [14].

Given lower and upper bounds (t_l, t_u) for job runtimes, Shmoys and Tardos present a 2-approximation algorithm that computes a schedule with communication cost at most C , and makespan at most 2τ ; as long as $t_l \leq t_{\mathcal{J}_{ij}} \leq t_u$. We assume these time bounds are given as input. To find an assignment that is at most 2τ , the algorithm performs a bisection search on the range of possible makespan values by keeping only those assignments with an objective function value less than half of the objective function value of the best assignment found thus far. The algorithm solves the linear program of the GA problem at most $\log(wP)$ times, where w is the total number

of jobs and P is the maximum workload among all jobs [19]. Among all the current assignments, we select the assignment with minimum makespan.

The initial workload distribution guarantees the makespan is at most 2τ provided $t_l \leq t_{\mathcal{J}_{tr}} \leq t_u, \forall t_{\mathcal{J}_{tr}}$, for given (t_l, t_u) . Changes among the fragments can imbalance the workload, and increase the makespan τ . To avoid excessive workload re-distributions, we define a *burstiness time buffer*, ζ , representing the allowable percentage change in job runtime due to workload bursts. We add ζ to (t_l, t_u) to define $t'_l = ((1 - \zeta) \cdot t_l)$, and $t'_u = ((1 + \zeta) \cdot t_u)$. If a job runtime, $t_{\mathcal{J}_{tr}}$, lies beyond (t'_l, t'_u) , M_c triggers a workload redistribution. In Section V-C, we study the overhead and frequency of re-distributions over real workloads for $\zeta = 0.1$ under varying rates of change, and found the overhead is about 6% of the total runtime.

B. Parallelized Incremental Temporal Matching

Another bottleneck is to compute the pattern matches over evolving and distributed fragments. We next introduce the procedures LocalVio and IncTED that efficiently maintain the matches in ParallelTED.

Incremental Local Matching. The local violation computation (Procedure LocalVio, line 4 of Algorithm ParallelTED) relies on fast computation of local pattern matches. At each superstep t , jobs are executed at each worker to compute matches of each query path Q_k corresponding to Q . For each Q_k in a joblet, it performs subgraph isomorphism matching on $\mathcal{G}(v', d)$ to find local matches. Matches that require edges from multiple workers are shipped to a single worker. The matches of Q are obtained by (1) taking the intersection of the nodes identified by the matches across all paths Q_k of Q , and (2) a verification to find true matches.

Coping with edge updates. New matches of Q_k can appear and existing matches disappear (or be updated) as changes occur to fragment F_{tr} . To adapt to these changes, we present an incremental matching strategy that avoids redundant computations, and tracks partial matches for each Q_k with their missing topological and literal conditions. We introduce a boolean vector $\bar{\beta}(h_i) = (b_1, \dots, b_{\kappa})$ over a candidate match h_i of Q in F_{tr} . $\bar{\beta}(h_i)$ contains κ components, where the k -th component is the matching status of $\omega_{trk}(Q_k, F_{tr}, \mathcal{G}(v', d))$. That is, if there exists a match h_i of Q_k in F_{tr} , then $\bar{\beta}(h_i) = 1$ (true), otherwise, $\bar{\beta}(h_i) = 0$ (false). In the latter case, a partial match h_i may be isomorphic to Q_k but not satisfy its literals. We define $\text{unSat}_k(h_i)$ as the set of unsatisfied literals $x' \in \bar{x}$ in h_i w.r.t. Q_k , e.g., $\text{unSat}_k(h_i) = \{x'.A = c \mid h_i(x').A \neq c\}$. We use $\bar{\beta}$ and unSat_k when h_i is clear from the context.

Each worker initializes and populates $\bar{\beta}$ and unSat_k as matches are found. As changes occur over the fragments, ParallelTED checks $\bar{\beta}$, and unSat_k to determine if new matches arise, and updates existing matches to minimize the need for (expensive) subgraph isomorphism operations. If

Algorithm 2: LMatch ($\mathcal{J}_{ij}, \mathcal{M}_r(Q, G_{i-1}), F_{ij}, c$)

```
1  $\mathcal{M}_r(Q, G_i) := \emptyset$ ;  
2 Initialize  $\bar{\beta}$  and  $\text{unSat}_k$  from  $\mathcal{M}_r(Q, G_{i-1})$ ;  
3  $\mathcal{M}_{chg} = \{h_{t_{i-1}}(\bar{x}) \in \mathcal{M}_r(Q, G_{i-1}) \mid c \text{ applied to } G_{t-1}\}$   
4 if  $c$  is insert/update ( $x.A = a$ ) then  
5   if  $b_k = 0$  and ( $x.A = a$ )  $\in \text{unSat}_k$  then  
6     Remove ( $x.A = a$ ) from  $\text{unSat}_k$ ;  
7     if  $\text{unSat}_k = \emptyset$  then  $b_k = 1$ ;  
8   else if  $b_k = 1$  and ( $x.A = b$ )  $\in Q_k$  then  
9     Add ( $x.A = b$ ) to  $\text{unSat}_k$ ;  $b_k = 0$ ;  
10 else if  $c$  is delete ( $x.A = a$ ) then  
11   if  $b_k = 1$  and ( $x.A = b$ )  $\in Q_k$  then  
12     Add ( $x.A = b$ ) to  $\text{unSat}_k$ ;  $b_k = 0$ ;  
13 else if  $c$  is insert ( $e$ ) then  
14   Add  $e$ , do subgraph isomorphism to evaluate  $b_k$ ;  
15   if  $c$  creates a new match for  $Q_k$  then  
16     Duplicate all vectors  $\bar{\beta}$  and set  $b_k = 1$ ;  
17 else if  $c$  is delete ( $e$ ) then  
18   if  $\bar{\beta}(h_i)[k] = 1$  then  
19      $b_k = 0$ ;  $\text{unSat}_k(h_i) = \emptyset$ ;  
20 foreach  $h_i \in \mathcal{M}_{chg}$  do  
21   if ( $\bar{\beta}(h_i)[k] = 1, \forall k$ ) then  
22      $\mathcal{M}_r(Q, G_i) += h_i$ ;  
23 return  $\mathcal{M}_r(Q, G_i)$ ;
```

the k -th component of $\bar{\beta}$ equals false, there are two cases to consider: (i) a topological match of Q_k exists, but there are unsatisfying literals in unSat_k ; or (ii) an empty unSat_k represents no topological match of Q_k in F_{tr} . For a job \mathcal{J}_{tr} , we evaluate the following cases for an input change c :

- (a) attribute insertion/deletion/update: we check whether c adds/removes literals from unSat_k , and update $\bar{\beta}$ to denote the insertion/deletion of a match h_i w.r.t. Q_k .
- (b) edge insertion: we perform subgraph isomorphism matching to determine whether a partial match is upgraded to a complete match w.r.t. Q_k .
- (c) edge deletion: if c causes a prior match h_i w.r.t. Q_k to be removed, we then set $\bar{\beta}(h_i)[k]$ to false, and add any unsatisfying literals to $\text{unSat}_k(h_i)$.

Algorithm 2 describes the details. For attribute updates, we update $\bar{\beta}$ and unSat_k without performing any subgraph isomorphism operations (Lines 4-12). For edge insertions, we perform subgraph isomorphism along Q_k to check for a new match (Lines 13-16). For edge deletions, which can only remove matches, we update b_k for Q_k (Lines 17-19). A match h_i of Q exists if $b_k = 1$ for all k , and we add h_i to $\mathcal{M}_r(Q, G_i)$ (Lines 20-22).

Example 6: Figure 2(b) shows (partial) matches of patterns Q'_1, Q'_2 . At t_1 , $\bar{\beta}(h_1)$ denotes no match of either Q'_1 nor Q'_2 , while $\bar{\beta}(h_1)[2]$ indicates a topological match of Q'_2 with non-empty unSat_2 containing literal $z = \text{McMaster}$. At t_2 , with an edge insertion labeled *study* from *Bob* to *Waterloo*,

Algorithm 3: IncTED ($\mathcal{G}_T, \sigma, \mathcal{M}(Q, G_t)$)

```
1  $\mathcal{E}(\mathcal{G}_T, \sigma) := \emptyset$ ;  
2 foreach  $h_i \in \mathcal{M}(Q, G_t)$  do  
3    $\{\Pi_X, \pi_{XY}\} := \{\Pi_X, \pi_{XY}\} \cup h_i$   
4    $\{\Gamma(\Pi_X), \Gamma(\pi_{XY})\} := \{\Gamma(\Pi_X), \Gamma(\pi_{XY})\} \cup i$ ;  
5    $\rho(i) := [\max(1, i - p), \min(i + q, T)]$ ;  
6   if  $\{\mu_X(h_j) \setminus \mu_X(h_i)\} \neq \emptyset, \forall j \in \rho(i)$  then  
7      $\mathcal{E}(\mathcal{G}_T, \sigma) := \mathcal{E}(\mathcal{G}_T, \sigma) \cup \{(h_i, i), (h_j, j)\}$ ;  
8   foreach ( $x.A = a$ )  $\in Y$  do  
9     if  $h_i.A \neq a$  then  
10     $\mathcal{E}(\mathcal{G}_T, \sigma) := \mathcal{E}(\mathcal{G}_T, \sigma) \cup \{(h_i, i)\}$ ;  
11 return  $\mathcal{E}(\mathcal{G}_T, \sigma)$ ;
```

we perform a subgraph isomorphism matching and find a topological match of Q'_1 . However, $\bar{\beta}(h_2(\bar{x}))$ remains false due to the unsatisfying *McMaster* literal in $\text{unSat}_1(h_2)$. Lastly, the update at t_3 to *University* from *Waterloo* to *McMaster* clears all unsatisfying literals, and updates $\bar{\beta}(h_3)$ to true for Q'_1 and Q'_2 , without requiring any additional matching. \square

Validating each $\sigma \in \Sigma$ may require us to store and pairwise compare all the local and cross-worker matches. We next introduce procedure IncTED, an Incremental TGFD Error Detection algorithm. The algorithm avoids the need to store the matches, and reduces the cost of the exhaustive pairwise match comparisons by performing efficient set difference operations.

Permissible Ranges. Rather than exhausting the comparison of any pair of matches, IncTED verifies match pairs with respect to a “current” time, $c = i$, and induces an allowable time range between h_i and h_j as defined by Δ . We define I_{h_i} and I_{h_j} as follows:

$$I_{h_i} = [1, |T| - p]$$
$$I_{h_j} = [(i + p), j'], \text{ where } j' = \begin{cases} T, & (i + q) > T \\ (i + q), & \text{o.w.} \end{cases} \quad (1)$$

If matches h_i, h_j have the same values in X , we want to identify matches h_j to compare against h_i by defining the allowable time range. We call this $\rho(i)$, the *permissible range* of h_i , as $\rho(i) = \{j \mid |j - i| \in \Delta\}$.

Auxiliary Structures. IncTED uses the following notations and auxiliary structures. To avoid enumeration of all pairwise matches in $\rho(i)$, we define a hash map, $\Pi_X(i)$, that partitions all matches of Q according to their values in X up to and including i . Specifically, let $\Pi_X = \{h_j \mid h_i.A = h_j.A, \forall (h_i.A, h_j.A) \in X, i \leq j\}$. We simply use Π_X when i is clear from the context. We sub-partition the matches in Π_X according to their distinct values in Y to identify error matches with different consequent values within the permissible range. We record the timestamps of such matches Π_X (resp. π_{XY}) in $\Gamma(\Pi_X)$ (resp. $\Gamma(\pi_{XY})$), i.e., $\Gamma(\Pi_X) = \{j \mid h_j \in \Pi_X\}$. We define a mapping function that returns the π_{XY} partition in which h_i belongs as $\mu_X(h_i) = \pi_{XY}$ such that $h_i \in \pi_{XY}$. For example, Figure 1(b) shows matches of σ with $\Pi_X = \{h_1, \dots, h_6\}$, $\Gamma(\Pi_X) = \{t_1, \dots, t_6\}$, and

Algorithm 4: LocalVio ($F_{ij}, \mathcal{J}_{ij}, t_i$)

- 1 $\mathcal{E}_r(F_r, \Sigma) := \emptyset$;
- 2 Initialize $\Pi_X, \pi_{XY}, \Gamma(\Pi_X), \Gamma(\pi_{XY})$;
- 3 Compute matches and errors over G_1 ;
- 4 $(\mathcal{M}_r(Q, G_1), h_{t_i}(\bar{x})) := \text{IsoUnit}(Q, G_{t_1})$
- 5 $\mathcal{E}_r(F_r, \Sigma) += \text{IncTED}(G_1, \sigma, \mathcal{M}_r(Q, G_1), \Pi_X, \pi_{XY}, \Gamma(\Pi_X), \Gamma(\pi_{XY}))$;
- 6 Compute matches and errors over subsequent $G_i, i \geq 2$
- 7 $\mathcal{M}_r(Q, G_i) = \emptyset$;
- 8 **foreach** $c \in \text{changes}$ **do**
- 9 $\mathcal{M}_r(Q, G_i) += \text{LMatch}(\mathcal{J}_{ij}, \mathcal{M}_r(Q, G_{i-1}), c)$;
- 10 $\mathcal{E}_r(F_r, \Sigma) += \text{IncTED}(F_{ij}, \Sigma, \mathcal{M}_r(Q, G_i), \Pi_X, \pi_{XY}, \Gamma(\Pi_X), \Gamma(\pi_{XY}))$;
- 11 Send $\mathcal{M}_r(Q, G_i), \mathcal{E}_r(F_r, \Sigma)$ to M_c

$\pi_{XY} = \{\{h_1, \dots, h_5\}\{h_6\}\}$, $\Gamma(\pi_{XY}) = \{\{t_1, \dots, t_5\}\{t_6\}\}$. These global structures and variables are maintained by the coordinator M_c and shared among all workers.

Algorithm. The algorithm IncTED is illustrated in Algorithm 3. After initializing the local error set (line 1), it iterates over the local matches and records the timestamps of each match in the auxiliary structures (lines 3-4). For each match h_i , the $\rho(i)$ is bookkept based on the timestamp of h_i (line 5). For variable TGFDs, if there exists another match h_j within the permissible range of h_i such that h_i and h_j have different set of timestamps for π_{XY} , then IncTED adds the pair to the violation set (lines 6-7). For constant TGFDs, if the match h_i violates a constant literal in Y , then it adds h_i to the violation set (lines 8-10).

Using IncTED algorithm, each worker computes its local set of errors, $\mathcal{E}_r(F_r, \sigma)$. For matches that span two workers, the coordinator verifies matches $h_i, h_{i'}$ from $M_r, M_{r'}, r \neq r'$, respectively. This is done by selecting matches from $\mu_X(h_i) = \pi_{XY}(h_i)$ and $\mu_X(h_{i'}) = \pi_{XY}(h_{i'})$ such that $|i - i'| \in \Delta$, and computing $\{\mu_X(h_{i'})\} \setminus \{\mu_X(h_i)\}$, i.e., checking whether the set difference is non-empty. If so, we add $\{(h_i, i), (h_{i'}, i')\}$ to the cross-machine error set $\mathcal{E}_c(\mathcal{G}_T, \Sigma)$. At each timestamp, we update $\mathcal{E}(\mathcal{G}_T, \Sigma)$ with $\mathcal{E}_c(\mathcal{G}_T, \Sigma) \cup_r \mathcal{E}_r(F_r, \Sigma)$. The incremental strategy improves the efficiency of a batch counterpart for TGFD-based error detection by 3.3 times (see Section V).

Algorithm 4 provides details of the matching and local error detection at each M_j . We compute matches and errors over the first graph snapshot G_1 (Lines 4-5), and then incrementally compute matches (Line 9), and errors (Line 10) via LMatch and LError, respectively. The set of local matches and errors for each M_j are sent to M_c (Line 11). Algorithm 1 shows ParallelTED which first estimates the jobs and communication cost before assigning jobs to the machines (Lines 4-7). At each t_i , M_c sends the changes (computed from log files) to all machine workers. Each M_j runs Algorithm 4 to compute matches and the local error set, which is sent to the coordinator

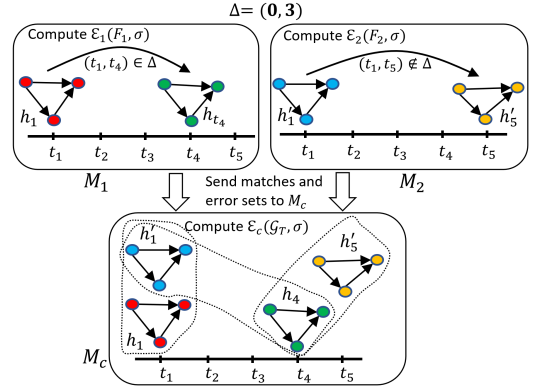


Fig. 3: Error detection in ParallelTED

node after each timestamp to minimize idle time at M_c (Lines 8-11). Lastly, M_c computes errors between M_j, M'_j by comparing matches from M'_j (Line 13) with those from M_j (Lines 14-15), and returns the total error set (Line 16).

Example 7: Figure 3 shows matches $\{h_1, h_4\}$ and $\{h'_1, h'_5\}$ for a σ with $\Delta = (0, 3)$ computed locally (via LMatch [14]) at M_1 and M_2 , respectively. M_1 computes local error set \mathcal{E}_1 via IncTED, and $\mathcal{E}_2 = \emptyset$ since $|t_5 - t_1| \notin \Delta$. M_c receives $\{h_1, h'_1\}, \{h_4, h'_1\}, \{h_4, h'_5\}$, validates the pairs (shown by dotted lines) via IncTED, and adds the violations to $\mathcal{E}(\mathcal{G}_T, \sigma) += \mathcal{E}_c(\mathcal{G}_T, \sigma) \cup \mathcal{E}_1$. \square

Runtime Analysis. In Algorithm 1, GenAssign runs in polynomial time taking at most 2τ to assign joblets [19]. The initial subgraph matching dominates the runtime (LocalVio) as an exponential number of subgraphs may match Q for each σ . Fortunately, subsequent, incremental matching takes linear time proportional to the number of changes at each worker due to our K -Path decomposition. Since $|Q|$ is small in practice, and we localize the matching to small graphs making it less likely to find exponentially many isomorphic subgraphs. At each superstep t , incremental violation detection (IncTED) runs in linear time w.r.t. the number of matches in G_t .

V. EXPERIMENTS

We evaluate our algorithms to test: (1) its scalability and impact of varying parameters; (2) the comparative effectiveness of TGFD-based error detection; and (3) case study that verifies real-world TGFDs and errors that can be captured.

A. Experimental Setup

Datasets. We use two real, and one synthetic graph. All datasets and source code are publicly available at [20].

- (1) **DBpedia** [21]: The graph contains in total 2.2M entities with 73 distinct entity types, and 7.4M edges with 584 distinct labels from 2015 to 2016, with snapshots every 6 months.
- (2) **IMDB** [22]: The data graph contains 4.8M entities with 8 types and 16.7M edges. IMDB provides diff files, where we extract 38 monthly updates from Oct. 2014 to Nov. 2017.
- (3) **PDD** [23]: The graph contains over 4.2M entities, 10.2M edges describing patient, drug, disease, and prescriptions. We

extracted 31 consecutive daily snapshots, and defined (with domain expertise) 12 TGFs, as reported in [20].

(4) Synthetic: We use the gMark benchmark [24], and generate data graphs with up to 21M vertices, 40M edges, and 11 attributes per node. We transform the static graph into a temporal graph of T timestamps by randomly generating updates 4% the size of the graph (*w.r.t.* the number of edges) to create subsequent graph snapshots.

TGFs Generation. We generated 40 TGFs (DBpedia, IMDB), and 20 TGFs (Synthetic) by using a discovery algorithm in our pilot study [12]. The discovery algorithm mines minimal and frequent k -bounded TGFs. We set the support level to find strict, and approximate TGFs that allow for exceptions. We consider matches with the most frequent consequent values as the ground truth. Lower support values lead to more exceptions and error values, and larger k lead to a larger number of expressive TGFs with more literals. We rank the TGFs according to decreasing support, and select the top-40 (20 for Synthetic). The pattern size, time intervals and size of TGFs are reported in Table II.

Comparative Baselines. We implemented the following.

(1) NaiveTED: We compute matches at each snapshot using the VF2 matching algorithm [25]. We verify matches between two snapshots if their time intervals lie within Δ .

(2) SeqTED: We implement a sequential TGF error detection algorithm by running IncTED on a single machine. We compute matches by using an incremental subgraph isomorphism matching algorithm, IsoUnit [16]. We run SeqTED on a Linux machine with AMD 2.7 GHz, 256GB RAM.

(3) GFD-Parallel: We implement the parallel GFD error detection algorithm [1]. For a set of GFDs Σ_{GFD} (defined in [20]), we compute matches for each $\varphi \in \Sigma_{\text{GFD}}$ over each G_i , and check whether $G_i \models \Sigma_{\text{GFD}}$ (pairwise matches between snapshots are not compared).

(4) GTAR-SubIso: Given a set of TGFs Σ , we transform each $\sigma \in \Sigma$ to a GTAR. We remove the $X \rightarrow Y$ dependency, and define a Δt time interval $(0, q)$, for a pattern Q (serving as both the antecedent and consequent) containing the same constants for each literal in \bar{x} . We evaluate this class of subgraph isomorphism-based GTARs for its error detection accuracy and performance.

Error Injection, Parameters, and Metrics. We inject positive and negative errors according to varying error rates. For instance, for positive errors, we randomly select $\text{err}\%$ of pairwise matches with equal values in X , and update their values in Y to create violations, and add the pair to the set of positive errors Γ^+ . For negative errors, we similarly pick $\text{err}\%$ of pairwise matches *w.r.t.* a TGF σ , and update a value in Y to a value in the domain of X' *w.r.t.* another TGF σ' , where $\{Y \cap X' \neq \emptyset\}$, and add to Γ^- .

We use the following commonly adopted measures:

TABLE II: Parameter values (defaults in bold)

Symbol	Description	Values
$ \Sigma $	#TGFs	10 , 20, 30, 40 (IMDB, DBpedia), 12 (PDD) 20 (Synthetic)
$ Q $	graph pattern size	2, 4, 6 , 8, 10
Δ	time interval	5, 10 , 15, 20, 25 month (IMDB)
T	total timestamps	5, 10 , 15, 20 (Synthetic)
$ G = (V , E)$	graph size (in M)	(5, 10) , (10, 20), (15, 30), (20, 40)
chg	change rate	2%, 4% , 6%, 8%, 10%
err (\mathcal{G}_T)	error rate	1%, 3% , 5%, 7%, 9%
n	#processors	2, 4 , 8, 16

$$\text{precision} = \frac{|\mathcal{E}(\mathcal{G}_T, \Sigma) \wedge \Gamma^+|}{|\mathcal{E}(\mathcal{G}_T, \Sigma)|} \text{ and } \text{recall} = \frac{|\mathcal{E}(\mathcal{G}_T, \Sigma) \wedge \Gamma^+|}{|\Gamma^+|}.$$

$$\text{The false positive rate is computed as } \text{fpr} = \frac{|\mathcal{E}(\mathcal{G}_T, \Sigma) \wedge \Gamma^-|}{|\Gamma^-|},$$

$$\text{and } F_1 = 2 \times \frac{\text{precision} \times \text{recall}}{\text{precision} + \text{recall}}.$$

Table II summarizes the parameters and their default values.

Implementation. We implement all our algorithms using Java v.13 and Scala. We run the tests on a cluster of 16 Amazon EC2 Linux machines, each with 32GB RAM, 8 cores at 2.5 GHz. The full set of data constraints including TGFs, source code, and datasets are available at [20].

B. Exp-1: Scalability

Vary $|\Sigma|$: Figure 4(a) and Figure 4(b) show ParallelTED outperforms SeqTED by an average 170%, with larger gains in IMDB (more graph snapshots). We stopped executions of NaiveTED over IMDB after 22hrs. ParallelTED runs 22% and 29% faster than GFD-Parallel over DBpedia and IMDB, respectively, despite having to evaluate more matches. This highlights the effectiveness of IncTED, and maintaining query path matches in the presence of changes.

Vary $|Q|$. Figure 4(c) and Figure 4(d) show that larger graph patterns incur higher runtimes as the cost of local pattern matching increases. This is especially evident for sequential algorithms NaiveTED and SeqTED. ParallelTED is 80% and 18% faster than SeqTED and GFD-Parallel, respectively.

Vary Δ . We found the performance of NaiveTED is sensitive due to the increased number of pairwise matches that need to be compared for larger Δ . In contrast, SeqTED and ParallelTED are largely insensitive due to their incremental checking strategies. Figure 4(e) shows the results.

Vary chg. Figure 4(f) shows SeqTED and ParallelTED runtimes increase by 27% and 26%, respectively, for increased changes. SeqTED uses IsoUnit to compute matches which become more expensive as the number of changes localized to a subgraph increases. ParallelTED uses boolean vectors to track changes to existing matches to avoid isomorphic computations (Section IV-B), and achieves the fastest runtime.

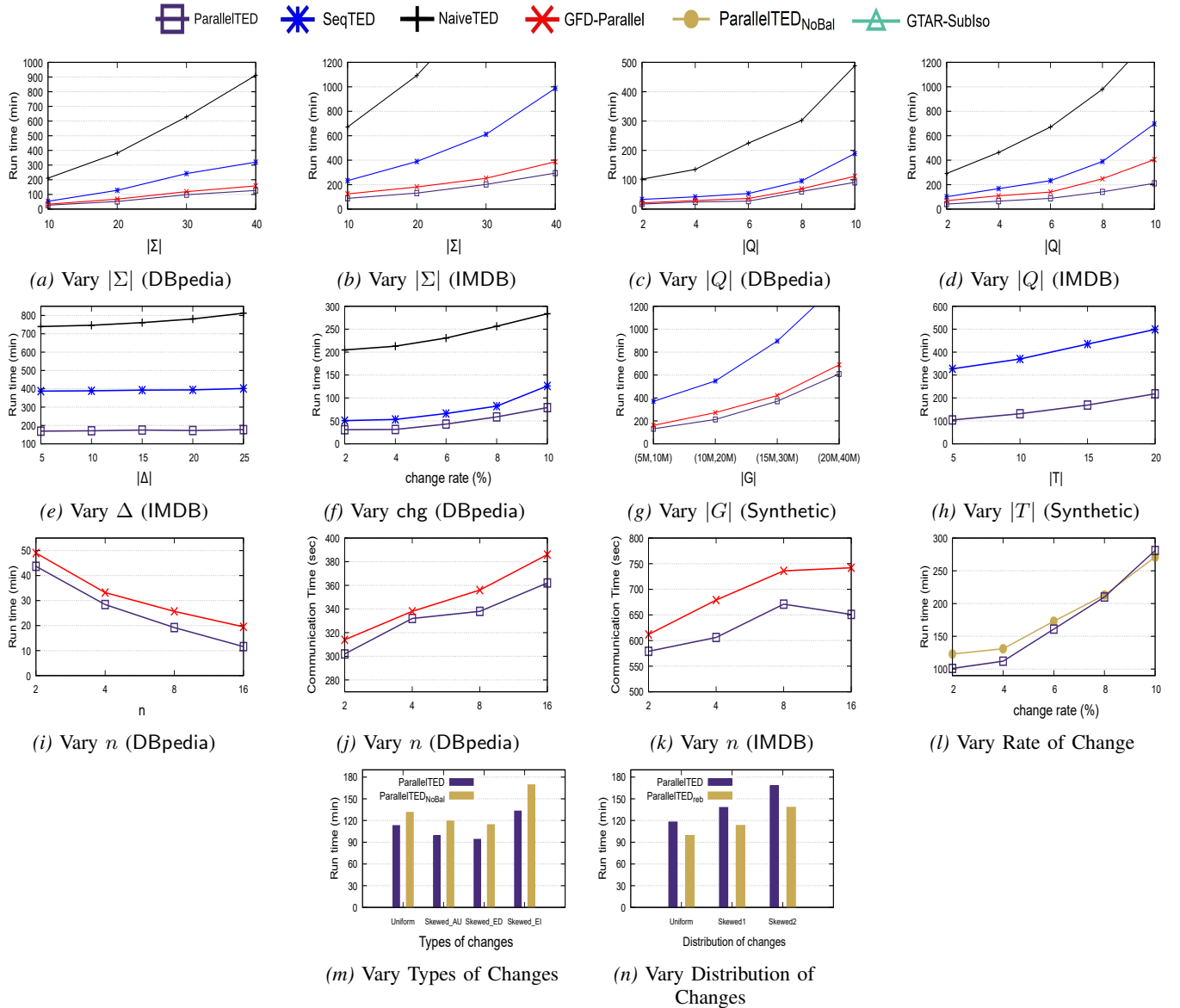


Fig. 4: TGFED error detection efficiency and effectiveness.

Vary $|G|$. Figure 4(g) shows that for increasingly large graph sizes, sequential algorithms are not feasible, i.e., we stopped SeqTED after 20hrs due to its exponential growth. However, ParallelTED shows that error detection is feasible over large graphs, outperforming GFD-Parallel by 18%.

Vary T . Figure 4(h) shows linear scaleup for increasing T . For larger T , we expect more matches to occur (assuming changes are spread uniformly), and validating a new match vs. existing matches in π_{XY} can be done in constant time.

Vary n . Figure 4(i) shows ParallelTED runs 29% faster than GFD-Parallel despite evaluating matches both within and between graph snapshots. IncTED's efficiency avoids redundant pairwise comparisons, and adaptively tunes matches to avoid expensive subgraph isomorphism computations.

Communication Overhead. Figures 4(j) and 4(k) show the communication overhead for an increasing number of workers, n . Using DBpedia and IMDB, the communication cost comprises between 10-48%, and 5-28%, respectively, of the total error detection time. As expected, for larger n , we see that both ParallelTED and GFD-Parallel incur increased overhead as the need to exchange data increases.

C. Exp-2: Adapting to Workload Changes

Rate of Change. We study the impact of the burstiness time buffer ζ by generating a graph of size (5M,10M), and implement a version of ParallelTED without ζ (no workload rebalancing) called ParallelTED_{NoBal}. Figure 4(l) shows ParallelTED runtimes with $\zeta = 0.1$ performs 16% faster as change rates less than 8% are accounted for by the burstiness

buffer, requiring only at most two workload re-distributions. Beyond this change point, larger ζ values are needed, which require more frequent workload re-distributions (up to six), and incur approximately 6% overhead.

Vary Type and Distribution of Changes. Using the same generated graph, we distribute changes according to: (i) a Uniform distribution that assigns attribute updates (AU) (40%), edge deletions (ED) (30%), and edge insertions (EI) (30%); (ii) each of Skewed_AU, Skewed_ED, Skewed_EI assigns 85% of changes to their respective type, and 7.5% to the other two types. Figure 4(m) show that EI are slowest as pattern matching becomes more expensive to find new matches. AU cause matches to be added/removed, and are slower compared to ED, which only lead to fewer matches. Across all change types, Figure 4(m) shows ParallelTED is 20% faster, on average, than ParallelTED_{NoBal}. We also evaluated data partitioning schemes such that hot spots are: (i) uniform across four nodes; (ii) 80% of hot spots across two nodes; and (iii) 70% on a single node. As expected, ParallelTED incurs 13% more time, compared to ParallelTED_{NoBal} at +19% (Figure 4(n)).

D. Exp-3: Comparative Performance

Comparing with GFDs and GTARs. Figures 5(a)-5(c) show the F_1 -score of ParallelTED against GFD-Parallel and GTAR-Sublso for varying error rates over the IMDB, DBpedia, and PDD datasets. ParallelTED outperforms GFD-Parallel and GTAR-Sublso on IMDB by an average of 55% and 74%, respectively. Over DBpedia (resp. PDD), ParallelTED achieves an average gain over GFD-Parallel and GTAR-Sublso of 20% and 48% (resp. 60% and 73%). GFD-Parallel achieves 23% recall using IMDB, while TGFs capture more errors “across” graph snapshots than GFDs. GFDs exhibit greater sensitivity to negative errors and false positives for increasing error rates as more match pairs are incorrectly detected as violations when temporal intervals are not considered. In comparison to GTAR-Sublso, with an average recall of 12%, TGFs have greater expressive power with variable and constant literals, to capture errors with non-zero lower bounds, and detect historical errors located in “past” matches. We found approximately 70% and 60% of detected violations are missed if using GTARs, and GFDs, respectively. ParallelTED achieves lower runtimes than GFD-Parallel and GTAR-Sublso on IMDB by (32%, 119%), DBpedia (67%, 140%), and PDD (73%, 151%), respectively (Figure 5(d)-Figure 5(f)).

E. Case Study: Example TGFs

We profiled DBpedia and PDD datasets to identify TGFs, and to validate their prevalence, and errors in real data [12]. **TGFD 1:** Figure 6(a) shows pattern Q_{ts} for $\sigma_{ts} = (Q_{ts}[\bar{x}], (1, 365), [x.name, y.season, z.name] \rightarrow [w.actor])$, which specifies “if a TV series in a given season is broadcast over a one-year period with a character role, then the actor playing this role must be unique.” Figure 6(d) shows a violation in Season 3 of the series *Trollhunters: Tales of Arcadia*, where character *Jim Lake Jr.* was first played by *Anton Yelchin*

in May 2018, and then by *Emile Hirsch* in Dec. 2018.

TGFD 2: Figure 6(b) shows Q_{sp} for $\sigma_{sp} = (Q_{sp}[\bar{x}], (1, 4), [x.name] \rightarrow [y.league, z.team])$ that states “a football player must play for the same team and league between one and four months in a given year.” Figure 6(e) shows a violation for player *Gareth Bale* who played for *Tottenham Hotspur* on Sep. 2020, and then transferred to *Real Madrid* on Nov. 2020.

TGFD 3: We profiled the PDD dataset, and Figure 6(c) shows pattern Q_{pt} (with only the blue vertices) for $\sigma_{pt} = (Q_{pt}[\bar{x}], (1, 7), [x.age, y.gender, v.name, u.name] \rightarrow [w.dose])$. TGFD σ_{pt} specifies “for any two patients of the same age, gender, disease and prescribed drug, they must take the same daily dosage over seven days.” We found that for 1323 patients with hypertension, 21% were taking inconsistent dosages of the drug *Metoprolol* ranging from 5mg to 100mg.

TGFD 4: We define pattern Q'_{pt} by augmenting Q_{pt} with an edge from *prescription* (q) to *duration* (z) (shown as a dotted edge in Figure 6(c)). Consider TGFD $\sigma'_{pt} = (Q'_{pt}[\bar{x}], (1, 31), [x.age, y.gender, v.name, u.name, w.dose] \rightarrow [z.duration])$ that specifies “For patients with the same age, gender, disease, drug, and dosage, the drug must be taken over the same duration of days.” However, we found that 41% of patients were taking their drug dosages over inconsistent durations ranging from 0 to 14 days.

VI. RELATED WORK

Graph Dependencies. GEDs [10] extend GFDs via literal equality of *entity id* over two nodes in the graph pattern to subsume GFDs and GKeys. GKeys and their ontological variants are defined to uniquely identify entities [2], [3]. NGDs [26] are defined to extend GFDs with the support of linear arithmetic expressions and built-in comparison predicates. None of these dependencies are applicable to catch inconsistencies over temporal graphs. TGFs use a time duration bound to induce the scope of historical and future matches relative to a current time. Association rules GPAR [4] are defined over static graphs. GTARs are soft rules for predictive analysis, and are unable to capture inconsistencies, particularly rare occurrences, across a given time duration.

Temporal Dependencies. FDs over temporal databases include *Dynamic Functional Dependencies* (DFDs) that hold over consecutive snapshots (states) of a database, where attribute values from a current state determine values in the next state, e.g., a new salary is determined by the last salary and the last merit increase [27]. Wijzen et. al., define *Temporal Functional Dependencies* (TFDs) that rely on object identity, include a valid-time on tuples, and apply to the sequence of snapshots defining a temporal relation [28]. DFDs constrain pairs of adjacent states, while TFDs constrain a sequence of multiple valid-time states. TGFs impose topological constraints that are not captured in relational settings, and TGFs model a different matching and temporal semantics. DFDs and TFDs impose consistency over tuples from adjacent snapshots. TGFs are not restricted to compare consecutive matches, but constrain the time difference of matches to lie within

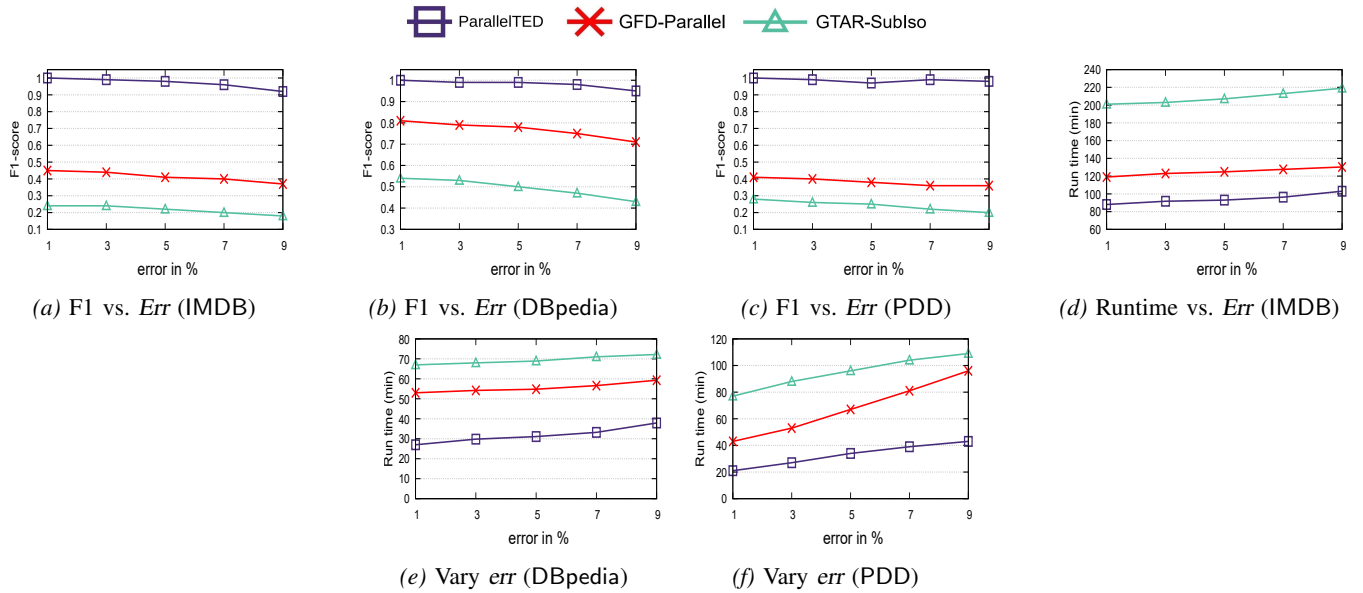


Fig. 5: Baseline comparative performance.

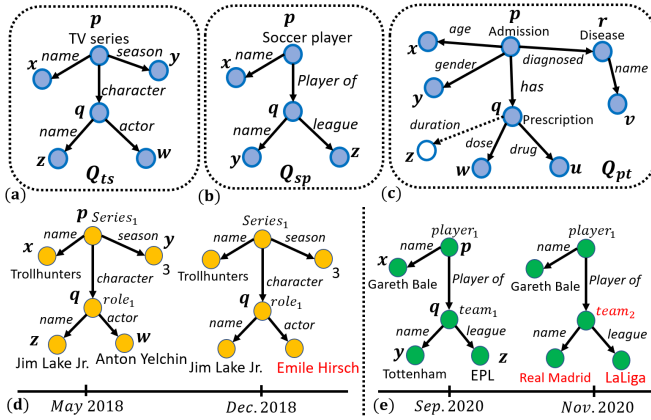


Fig. 6: Case study: TGFDs in real-world graphs.

the Δ interval. Second, TGFDs model the time interval duration when topological and attribute consistency is expected, whereas DFDs and TFDs do not model such semantics.

Temporal Graph Mining. Frequent dynamic subgraphs discover patterns beyond a given threshold over a time interval [29]. Mining temporal motifs capture dynamic interactions with patterns [30], [31], with extensions to time windows [31]. Mining algorithms identify dense temporal cliques with partitioning schemes over temporal graphs [32], MDL-based approaches to identify associations between changes [33], and mining for cross-graph quasi-cliques [34]. While our work shares a similar spirit to identify consistent temporal patterns, TGFDs impose attribute dependency and temporal constraints over identified matches of a given pattern.

Constraint-Based Graph Cleaning. There has been extensive work to infer missing data in graphs [35]. [36] proposed a constraint based approach to infer missing data in graphs.

Graph Quality Rules (GQRs) [37] are defined to deduce *certain* fixes over graphs by supporting conditional functional dependencies, graph keys and negative rules. These techniques are designed for static graphs to suggest changes or provide provenance information based on enforcing a set of rules. TGFDs serve a different purpose to model time-dependent data consistency requirements over temporal graphs that are conditioned by a given time interval.

VII. CONCLUSION

We proposed TGFDs, a class of graph dependencies that characterize errors induced by graph patterns and time intervals for temporal graphs. We established complexity results for fundamental problems, and introduced a sound and complete axiom system. We introduced a parallel, and an incremental algorithm for TGFD-based error detection. Our experimental results verified the effectiveness and efficiency of our error detection algorithms. As next steps, we intend to explore non-parametrized methods to extend our workload rebalancing scheme to adapt to workload burstiness. Graph data cleaning with respect to TGFDs would also be an interesting next step.

REFERENCES

- [1] W. Fan, Y. Wu, and J. Xu, "Functional dependencies for graphs," in *SIGMOD International Conference on Management of Data*, 2016, pp. 1843–1857.
- [2] W. Fan, Z. Fan, C. Tian, and X. L. Dong, "Keys for graphs," *Proceedings of the VLDB Endowment*, vol. 8, no. 12, pp. 1590–1601, 2015.
- [3] H. Ma, M. Alipourlangouri, Y. Wu, F. Chiang, and J. Pi, "Ontology-based entity matching in attributed graphs," *Proceedings of the VLDB Endowment*, vol. 12, no. 10, pp. 1195–1207, 2019.
- [4] W. Fan, X. Wang, Y. Wu, and J. Xu, "Association rules with graph patterns," *Proceedings of the VLDB Endowment*, vol. 8, no. 12, pp. 1502–1513, 2015.
- [5] X. Wang, Y. Xu, and H. Zhan, "Extending association rules with graph patterns," *Expert Systems with Applications*, vol. 141, p. 112897, 2020.

- [6] (2021) Canada's COVID-19 economic response plan. [Online]. Available: <https://www.canada.ca/en/departement-finance/economic-response-plan.html#businesses>
- [7] (2020) Fda approves first treatment for COVID-19. [Online]. Available: <https://www.fda.gov/news-events/press-announcements/fda-approves-first-treatment-covid-19>
- [8] P. Augustyniak and G. Slusarczyk, "Graph-based representation of behavior in detection and prediction of daily living activities," *Computers in Biology and Medicine*, vol. 95, pp. 261–270, 2018.
- [9] (2022) Institute for safe medication practices, fda advise-err: Reported medication errors with veklury (remdesivir) emergency use authorization. [Online]. Available: <https://www.ismp.org/resources/fda-advise-err-reported-medication-errors-veklury/remdesivir-emergency-use-authorization>
- [10] W. Fan and P. Lu, "Dependencies for graphs," *ACM Transactions on Database Systems (TODS)*, vol. 44, no. 2, pp. 1–40, 2019.
- [11] M. H. Namaki, Y. Wu, Q. Song, P. Lin, and T. Ge, "Discovering graph temporal association rules," in *CIKM*, 2017, pp. 1697–1706.
- [12] L. Noronha and F. Chiang, "Discovery of temporal graph functional dependencies (short paper)," in *CIKM, Virtual Event*, 2021, pp. 3348–3352.
- [13] J. Wijsen, "Temporal dependencies," in *Encyclopedia of Database Systems*, 2009.
- [14] M. Alipourlangouri, A. Mansfield, F. Chiang, and Y. Wu, "Temporal graph functional dependencies, extended version," 2022. [Online]. Available: <https://arxiv.org/abs/2108.08719>
- [15] M. R. Garey and D. S. Johnson, *Computers and Intractability: A Guide to the Theory of NP-Completeness*. W. H. Freeman and Co., 1990.
- [16] W. Fan, J. Li, J. Luo, Z. Tan, X. Wang, and Y. Wu, "Incremental graph pattern matching," in *Proceedings of the 2011 ACM SIGMOD International Conference on Management of Data*, 2011, p. 925–936.
- [17] T. Bleifuß, L. Bornemann, T. Johnson, D. V. Kalashnikov, F. Naumann, and D. Srivastava, "Exploring change: A new dimension of data analytics," *Proc. VLDB Endow.*, vol. 12, no. 2, p. 85–98, Oct. 2018.
- [18] E. P. Shironoshita, M. T. Ryan, and M. R. Kabuka, "Cardinality estimation for the optimization of queries on ontologies," *SIGMOD Rec.*, vol. 36, no. 2, p. 13–18, 2007.
- [19] D. B. Shmoys and É. Tardos, "An approximation algorithm for the generalized assignment problem," *Mathematical programming*, vol. 62, no. 1, pp. 461–474, 1993.
- [20] (2022) TGFDF source code and data repository. [Online]. Available: <https://github.com/TGFDF-Project/TGFDF/>
- [21] J. Lehmann, R. Isele, M. Jakob, A. Jentzsch, D. Kontokostas, P. N. Mendes, S. Hellmann, M. Morsey, P. Van Kleef, S. Auer *et al.*, "DBpedia—a large-scale, multilingual knowledge base extracted from Wikipedia," *Semantic Web*, 2015.
- [22] "IMDB dataset," 2021. [Online]. Available: <ftp://ftp.fu-berlin.de/pub/misc/movies/database/frozendata/>
- [23] M. Wang, J. Zhang, J. Liu, W. Hu, S. Wang, X. Li, and W. Liu, "Pdd graph: Bridging electronic medical records and biomedical knowledge graphs via entity linking," in *International Semantic Web Conference*. Springer, 2017, pp. 219–227.
- [24] G. Bagan, A. Bonifati, R. Ciucanu, G. H. Fletcher, A. Lemay, and N. Advokaat, "Generating flexible workloads for graph databases," *Proceedings of the VLDB Endowment*, vol. 9, no. 13, pp. 1457–1460, 2016.
- [25] P. Foggia, C. Sansone, and M. Vento, "A performance comparison of five algorithms for graph isomorphism," in *Proceedings of the 3rd IAPR TC-15 Workshop on Graph-based Representations in Pattern Recognition*, 2001, pp. 188–199.
- [26] W. Fan, X. Liu, P. Lu, and C. Tian, "Catching numeric inconsistencies in graphs," in *SIGMOD*, 2018, pp. 381–393.
- [27] C. Jensen, R. Snodgrass, and M. Soo, "Extending existing dependency theory to temporal databases," *IEEE Transactions on Knowledge and Data Engineering*, vol. 8, no. 4, pp. 563–582, 1996.
- [28] J. Wijsen, J. Vandenbulcke, and H. Olivie, "Functional dependencies generalized for temporal databases that include object-identity," in *International Conference on the Entity-Relationship Approach*, ser. Lecture Notes in Computer Science, vol. 823, 1993, pp. 99–109.
- [29] K. M. Borgwardt, H.-P. Kriegel, and P. Wackersreuther, "Pattern mining in frequent dynamic subgraphs," in *Sixth International Conference on Data Mining (ICDM'06)*. IEEE, 2006, pp. 818–822.
- [30] S. Gurukar, S. Ranu, and B. Ravindran, "Commit: A scalable approach to mining communication motifs from dynamic networks," in *Proceedings of the 2015 ACM SIGMOD International Conference on Management of Data*, 2015, pp. 475–489.
- [31] A. Paranjape, A. R. Benson, and J. Leskovec, "Motifs in temporal networks," in *Proceedings of the tenth ACM international conference on web search and data mining*, 2017, pp. 601–610.
- [32] J. Sun, C. Faloutsos, S. Papadimitriou, and P. S. Yu, "Graphscope: parameter-free mining of large time-evolving graphs," in *Proceedings of the 13th ACM SIGKDD international conference on Knowledge discovery and data mining*, 2007, pp. 687–696.
- [33] J. Ferlez, C. Faloutsos, J. Leskovec, D. Mladenic, and M. Grobelnik, "Monitoring network evolution using mdl," in *2008 IEEE 24th International Conference on Data Engineering*. IEEE, 2008, pp. 1328–1330.
- [34] J. Pei, D. Jiang, and A. Zhang, "On mining cross-graph quasi-cliques," in *Proceedings of the eleventh ACM SIGKDD international conference on Knowledge discovery in data mining*, 2005, pp. 228–238.
- [35] H. Paulheim, "Knowledge graph refinement: A survey of approaches and evaluation methods," *Semantic web*, vol. 8, no. 3, pp. 489–508, 2017.
- [36] Q. Song, P. Lin, H. Ma, and Y. Wu, "Explaining missing data in graphs: A constraint-based approach," in *2021 IEEE 37th International Conference on Data Engineering (ICDE)*. IEEE, 2021, pp. 1476–1487.
- [37] W. Fan, P. Lu, C. Tian, and J. Zhou, "Deducing certain fixes to graphs," *Proceedings of the VLDB Endowment*, vol. 12, no. 7, pp. 752–765, 2019.